Polystyrene-*block*-poly(2-cinnamoylethyl methacrylate) Adsorption in the van der Waals−Buoy Regime

Jianfu Ding, Jian Tao, Andrew Guo, Sean Stewart, Nanxing Hu, Viola I. Birss, and Guojun Liu*

Department of Chemistry, The University of Calgary, 2500 University Drive, NW, Calgary, Alberta, Canada T2N 1N4

Received February 21, 1996; Revised Manuscript Received May 1, 1996[⊗]

ABSTRACT: Polystyrene-*block*-poly(2-cinnamoylethyl methacrylate) (PS-*b*-PCEMA) polymers of different asymmetric ratios, β, and numbers, m, of CEMA units were synthesized and characterized. In cyclopentane/THF mixtures, the polymers were adsorbed by silica mainly via the PCEMA block in the brush conformation. For samples with β values greater than 4, their surface adsorption data could be well explained by the theory of Marques et al. for diblock adsorption from micelle solutions in the van der Waals−buoy regime. This represents the first experimental confirmation of such a scaling relation. On silver surfaces, the PCEMA block was the main adsorbing species for samples with small β and large m, and both the PS and PCEMA blocks adsorbed for samples with large β and small m values. As polymer brushes are not formed from certain polymers, the data of polymer adsorption by silver did not follow the scaling relation of Marques et al.

I. Introduction

In a block-selective solvent, which is good for one block but poor for the other, a diblock copolymer may deposit on a solid substrate which contacts the polymer solution. If the interaction between the insoluble block and the solid substrate is favorable, a dense polymeric monolayer called a polymer brush may form. In a polymer brush, the insoluble block spreads on the solid surface like a melt and the soluble block stretches into the solution phase like bristles of a brush (Figure 1).[1−4]

There have been a few studies of diblock adsorption equilibrium in block-selective solvents.[5−9] Polymers studied include polystyrene-*block*-poly(2-vinylpyridine) (PS-*b*-PVP),[5−6] polyisoprene-*block*-poly(2-vinylpyridine),[7] polystyrene-*block*-poly(propylene sulfide),[8] and polystyrene-*block*-poly(2-cinnamoylethyl methacrylate) (PS-*b*-PCEMA).[9] In all previous studies except one,[9] the surface coverage ρ_∞, the number of chains adsorbed per unit substrate surface area, has been explained by the scaling relation derived by Marques et al.[10] for unimer adsorption in the van der Waals−buoy regime. That is, ρ_∞ increased with the asymmetric ratio β of a diblock copolymer defined by

$$\beta = n^{3/5}/m^{1/2} \tag{1}$$

where n and m represent the degree of polymerization for the soluble and insoluble block, respectively.

We recently studied the adsorption of PS-*b*-PCEMA samples with β close to 1 from cyclohexane/THF and cyclopentane/THF (CP/THF) mixtures, where cyclohexane and CP solubilize PS but not PCEMA.[9] At sufficiently high cyclohexane or CP contents, PS-*b*-PCEMA existed as micelles. Our experiments demonstrated that

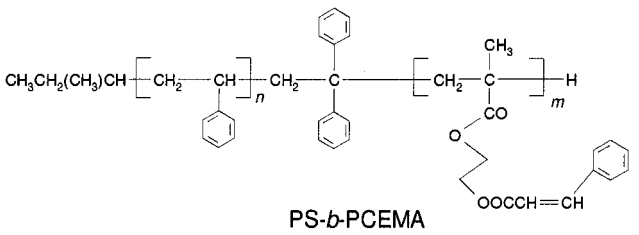

PS-*b*-PCEMA

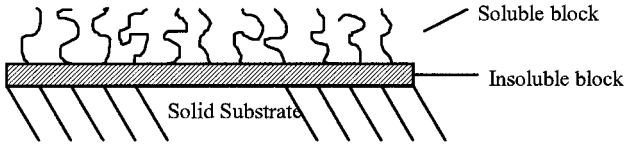

Figure 1. Polymer brush illustrated.

the adsorption of PS-*b*-PCEMA chains by silica from such solutions occurred via the anchoring of the PCEMA block in the brush conformation. Detailed analysis showed that our ρ_∞ data could be interpreted by the theory of Marques et al.[10] for block copolymer adsorption from a micellar solution in the buoy-dominated regime. That is,

$$\rho_\infty \propto m^{-(13/25)}\beta^{-2} \tag{2}$$

This represented the first experimental observation of such a trend.

The theory of Marques et al. also suggests that diblock copolymer adsorption behavior enters a new regime, i.e. the van der Waals−buoy regime, if β are made significantly larger than 1. In the van der Waals−buoy regime, ρ_∞ are given by

$$\rho_\infty \propto m^{-(17/23)}\beta^{-(10/23)} \tag{3}$$

This research was initiated to test the validity of this scaling relation if such a regime does exist. As 19 polymers with various β values were used, we also observed the crossover of our ρ_∞ data from the van der Waals−buoy regime to the buoy-dominated regime. In addition, we examined the effect of different substrates, silica versus silver, on PS-*b*-PCEMA adsorption.

II. Experimental Section

Polymer Synthesis and Characterization. The detailed procedure for synthesizing PS-*b*-PCEMA has been described elsewhere.[9,11] The polymers were synthesized by anionic polymerization. Styrene was polymerized at −78 °C in THF using *sec*-butyllithium. 1,1-Diphenylethylene (DPE) and lithium chloride, both at 3.0 equiv to *sec*-butyllithium, were then added. DPE reacted with polystyryl anions to convert them to the sterically more hindered PS−DPE anion. The presence of lithium chloride was supposed to improve the polydispersity of the second block. The second block was prepared by initiating the polymerization of (trimethylsiloxy)ethyl meth-

[⊗] Abstract published in *Advance ACS Abstracts,* July 1, 1996.

acrylate (TMSEMA) with PS−DPE anions. The trimethylsilyl protecting groups were removed by hydrochloric acid catalyzed hydrolysis of PS-*b*-PTMSEMA in a THF/methanol mixture to produce polystyrene-*block*-poly(2-hydroxyethyl methacrylate) (PS-*b*-PHEMA). To attach cinnamoyl groups, PS-*b*-PHEMA was reacted with cinnamoyl chloride in pyridine.

GPC analysis was done on a Varian Model 5000 HPLC instrument using a Styragel HR 4 (Waters) column calibrated by monodisperse polystyrene standards (Polymer Laboratories). The ratio of the number of styrene to CEMA units, n/m, was determined using ^{1}H NMR. The absolute weight-average molar masses were measured using a Brookhaven Model 9025 light scattering instrument.

We used two numbers separated by a hyphen to denote a PS-*b*-PCEMA sample, where the numbers before and after the hyphen stand for the numbers of styrene and CEMA units in a polymer calculated from the molar feeding ratios of monomers to initiator. It should be noted that the number of styrene or CEMA units in a polymer calculated from the molar monomer to initiator feeding ratio is normally smaller than the actual value. This difference becomes more pronounced as polymer molar masses increase, because the preparation of higher molar mass samples required less catalyst, which made the effect of a trace amount of impurity such as water present more visible by reducing the number of living chains and increasing the molar mass of the final polymer.

Adsorption Data. To prepare the coating solution, PS-*b*-PCEMA was first dissolved in THF. A given amount of CP (Aldrich, 95%) was then added to prepare a coating solution with a designated CP volume fraction, f_c. CP was used in preference to cyclohexane, as the Θ temperature of PS in CP is 20 °C. In cyclohexane, this value is 34.5 °C.

Nonporous Aerosil Ox 50 (Degussa) and silver-covered nickel spheres (Ag−Ni spheres, Alfa, 15% Ag, 85% Ni) were used as the adsorbents. Aerosil Ox 50 consisted essentially of primary spherical particles, 400 Å in diameter, with a small amount of chain-shaped aggregates. The specific surface area of Aerosil Ox 50 was reported by Degussa to be 50 m^2/g. Ag−Ni spheres were shown, under an optical microscope, to have an average diameter of 6.0 μm. Using the densities of 8.90 and 10.52 g/mL for Ni and Ag, we calculated a specific surface area of 0.11 m^2/g for Ag−Ni spheres. The adsorbents were evacuated just before use and stored in a desiccator when not in use.

For the determination of the equilibrium surface coverages, silica or Ag−Ni spheres were equilibrated with a coating solution for 48 h or longer. The silica or Ag−Ni spheres were then separated from the supernatant by centrifuging. The supernatant was diluted and analyzed for cinnamate content by UV absorbance measurements at 274 nm. The amount of polymer adsorbed by an adsorbent was calculated from the initial and final cinnamate absorbances, A_0 and A_t, by

$$w_a = \frac{A_0 - A_t}{A_0} c_0 V_0 \tag{4}$$

where c_0 and V_0 were the initial concentration and volume of the coating solution to which the adsorbent was added, respectively. The surface coverage, σ_{eq}, was calculated using

$$\sigma_{eq} = \frac{w_a}{A_{sp} w_s} \tag{5}$$

where w_s is the amount of adsorbent used, and A_{sp} is the specific surface area of the adsorbent in use.

When plotting σ_{eq} vs the concentration, c_{eq}, of a polymer solution which is in equilibrium with an adsorbent, one normally obtains curves like those shown in Figures 2 and 3. σ_{eq} thus initially increases sharply with c_{eq} and then levels off as c_{eq} is further increased. The σ_{eq} obtained after an isotherm levels off is denoted σ_∞. To compare the surface coverages of different polymers, we compare their σ_∞ values.

The isotherms of diblocks should, in principle, be constructed to determine their σ_∞ values. Instead, we used σ_{eq} determined for silica at $c_0 \cong 10$ mg/mL to approximate σ_∞, as σ_{eq} levels off at high c_{eq} or c_0 values. In our experiment, the amount of polymer adsorbed by ∼0.040 g of silica was determined after it was stirred for ∼48 h with 2.00 mL of a ∼10 mg/mL PS-*b*-PCEMA solution in CP/THF with $f_c = 0.86$. This led to σ_{eq} values typically ∼0.35 μg/cm^2 (Table 3) and c_{eq} normally ∼7 mg/mL. That σ_{eq} of silica actually leveled off for 400−50 and 330−23 at c_{eq} values less than 7 mg/mL is obvious from Figure 2. Our previous results[9] demonstrated that σ_{eq} leveled off at lower c_{eq} values for samples with larger m and smaller β values, in agreement with the trend observed for 400−50 and 330−23. Since most samples employed in this study have larger m and smaller β values than 330−23 does, we can expect the adsorption isotherms of our samples to level off when $c_0 \cong 10$ mg/mL.

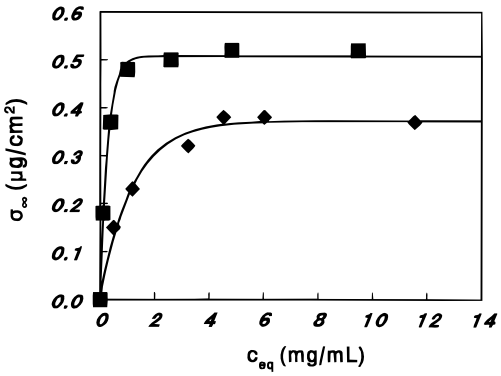

Figure 2. Isotherms of 330−23 (♦) and 400−100 (■) adsorption by silica from CP/THF with $f_c = 0.86$.

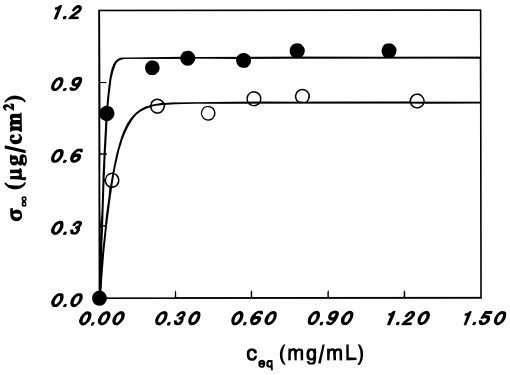

Figure 3. Isotherms of 330−23 (●) and 400−50 (○) adsorption by Ag−Ni spheres from CP/THF with $f_c = 0.96$.

In coating the silver, 0.40 g of Ag−Ni spheres was gently shaken with 2.00 mL of a PS-*b*-PCEMA solution in CP/THF ($f_c = 0.96$) at 25 °C. The initial coating solution concentration used was ∼1.0 mg/mL. Due to the low specific surface area of the Ag−Ni spheres, only ∼20% of the polymer was adsorbed and c_{eq} was thus ∼0.8 mg/mL. That c_{eq} leveled off at c_{eq} less than 0.8 mg/mL is obvious from Figure 3. The much lower leveling-off c_{eq} values were caused partially by the high f_c (0.96) value used compared to the silica-coating case where $f_c = 0.86$.

The surface coverage σ_∞ of each sample was determined in triplet. The data precision was within ±5%.

Surface-Enhanced Raman Spectroscopic (SERS) Studies. Silver foils (Aldrich, 0.025 mm thick, 99.9%) were roughened by dipping them in an aqueous mixture of 3 M nitric acid and 2 M sulfuric acid for 3−5 min. The foils were then rinsed with distilled water and dried with a gust of nitrogen. To coat the silver surfaces with a thin film of SiO_2, roughened silver foils were immersed in a 0.10 mg/mL tetraethyl orthosilicate (Aldrich, 98%) solution in 95% ethanol for 2 h and then dried in open air for 1 day.[12] A PS-*b*-PCEMA film on these substrates was obtained by equilibrating the substrate with a PS-*b*-PCEMA solution ($c = 2.0$ mg/mL, $f_c = 0.96$) for 2 h and then drying the withdrawn substrate surface by blowing nitrogen on it.

All SERS spectra were recorded on Jarrell-Ash Model 25-100 instrument. The slits were so set to provide a 5 cm^{-1} resolution. The excitation used was a 4-W argon ion laser

Table 1. Characterization of Polymers

lab code	(*n*/*m*) by NMR	$\bar{M}_w/\bar{M}_n$ by GPC	$\bar{M}_w$ by GPC (g/mol)	$\bar{M}_w$ by LS (g/mol)
800−60[a]	13.8	1.17	9.6×10^4	10.3×10^4
330−23	12.0	1.10	2.94×10^4	3.5×10^4
400−33	10.1	1.14	3.8×10^4	4.5×10^4
120−10	9.9	1.13	1.52×10^4	1.67×10^4
200−16[a]	9.7	1.30	2.69×10^4	3.1×10^4
1200−150[a]	9.6	1.24	24.8×10^4	25.4×10^4
1600−200[a]	9.4	1.30	20.7×10^4	29.8×10^4
260−22	9.2	1.09	2.49×10^4	2.79×10^4
400−50	8.2	1.10	3.3×10^4	4.2×10^4
800−100	7.9	1.12	14.8×10^4	17.1×10^4
600−75	7.0	1.12	10.0×10^4	11.0×10^4
400−67	6.8	1.09	5.0×10^4	7.2×10^4
250−45	5.3	1.08	3.0×10^4	3.6×10^4
400−100[a]	4.7	1.15	5.4×10^4	6.8×10^4
250−60[a]	3.5	1.19	4.1×10^4	5.0×10^4
800−200	3.5	1.08	18.5×10^4	23.7×10^4
600−150	3.2	1.09	9.7×10^4	16.7×10^4
200−50	3.1	1.10	3.1×10^4	4.3×10^4
300−150	1.82	1.08	5.2×10^4	6.9×10^4

[a] Samples with shoulders.

(Coherent) emitting at 514.5 nm. The incidence angle on SERS specimens was ~60° and the incident energy was ~80 mW at the sample. Silver foils were placed against a metal block to facilitate quick heat dissipation. Plasma lines were removed by placing a narrow-bandpass filter between the laser and the sample. SERS spectra of polymer films were obtained by subtracting the background spectrum of the bare substrate from those of polymer-coated substrates.

III. Results and Discussion

Polymer Characterization Results. The ^{1}H NMR spectrum of a PS-*b*-PCEMA sample was shown previously.[9] From the ratio of the peak intensity of PS to that of PCEMA, we obtained styrene to CEMA ratios, i.e. *n*/*m*, for all our samples, which are shown in Table 1.

GPC characterization suggests that the majority of our samples had low polydispersity indices or narrow molar mass distributions (Table 1). Since the GPC column was calibrated using monodisperse PS standards, the weight-average molar masses of the diblocks are included in Table 1 only to double check the light scattering results.

The method for determining the molar masses of diblocks by light scattering (LS) has been described in detail previously.[9,13] All samples were subjected to filtration through a GPC column before analysis by LS. Due to the difference in the refractive index increments of the two blocks of a diblock relative to that of toluene, the solvent used for LS measurement, the weight-average molar mass, $\bar{M}_w$*, measured following the method used for determining those of homopolymers is the apparent value. This value was corrected to obtain the true molar mass, $\bar{M}_w$, using

$$\frac{\bar{M}_w^*}{\bar{M}_w} = \frac{1}{\nu^2}[\nu_1\nu_2 - (\nu_1\nu_2 - \nu_2^2)w_{PS}^2 - (\nu_1\nu_2 - \nu_1^2)(1 - w_{PS})^2] \quad (6)$$

where ν_1 and ν_2, 0.938 and 0.112 mL/g, are the specific refractive index increments of PCEMA and PS, respectively; ν is that of the diblock. The values of ν shown in Table 2 were computed using an empirical relation established previously:[9]

$$\nu = 0.0938 + 0.0299w_{PS} - 0.0115w_{PS}^2 \quad \text{(mL/g)} \quad (7)$$

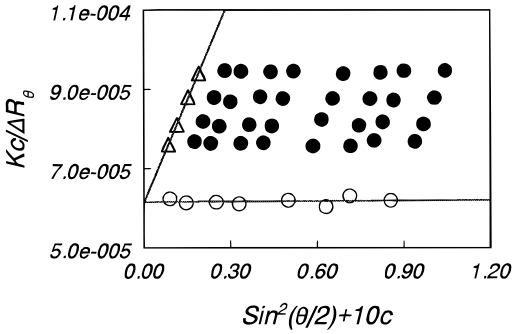

Figure 4. Zimm plot for 120−10. Experimental data are represented by solid circles. Triangles represent the concentration dependence of $Kc/\Delta R_\theta$. Linear regression analysis yields $Kc/\Delta R_\theta = 6.1 \times 10^{-5} + 1.73 \times 10^{-3}c$ (mol/g) with a correlation coefficient of 0.9998. Unfilled circles represent the angle dependence of $Kc/\Delta R_\theta$. Linear regression analysis yields $Kc/\Delta R_\theta = 6.2 \times 10^{-5} + 4.7 \times 10^{-7} \sin^2(\theta/2)$ (mol/g) with a correlation coefficient of 0.156.

where w_{PS} is the weight fraction of polystyrene in a diblock copolymer. Using *n*/*m* values determined from NMR and $\bar{M}_w$ from LS, the weight-average *n* and *m* values were calculated and are presented in Table 2.

As an illustration, the light scattering data of 120−10 are plotted in Figure 4. The apparent molar mass $\bar{M}$* for 120−10 determined from the Zimm plot was 1.63×10^4 g/mol. After correction using eq 6, the true molar mass was found to be 1.67×10^4 g/mol. The precision in the molar mass data was high. Due to the small slope for the $Kc/\Delta R_\theta$ vs $\sin^2(\theta/2)$ data, the radius of gyration, R_G, determined for this sample should have a large error margin. Thus, we included R_G values only for samples with relatively large molar masses in Table 2.

PS-*b*-PCEMA Adsorption on Silica via the PCEMA Block in a Block-Selective Solvent. In a previous study, we showed that silica adsorbed a negligible amount ($\sigma_\infty = 0.011$ μg/cm^2) of a PS homopolymer ($\bar{M}_w = 3.0 \times 10^4$ g/mol and $\bar{M}_w/\bar{M}_n = 1.05$) from a 90/10 cyclohexane/THF mixture.[9] In the present study, we determined a silica surface coverage value of 0.040 μg/cm^2 by PS (Polymer Laboratories, $\bar{M}_w = 9.0 \times 10^4$ g/mol, $\bar{M}_w/\bar{M}_n = 1.04$) from CP/THF with $f_c = 0.96$. We expect this surface coverage value to be even lower if $f_c = 0.86$ instead of 0.96. We determined the silica surface coverages at $f_c = 0.96$ to facilitate the comparison between the adsorption behavior of silica and silver.

Since PS does not adsorb significantly under our conditions used for coating silica, the adsorption of PS-*b*-PCEMA samples (Table 3) must have arisen via the anchoring of the PCEMA block. Further evidence suggesting the selective adsorption of PCEMA by silica under our conditions was obtained from surface-enhanced Raman spectroscopic (SERS) studies of PS-*b*-PCEMA films formed on SiO_2-coated silver foils based on the principle that an adsorbed functional group should display a stronger SERS signal.[14,15] When a 260−22 film was prepared on a SiO_2-coated silver foil by soaking the foil in a 260−22 solution in CP/THF with $f_c = 0.86$ for 2 h and drying the withdrawn foil surface with a gust of nitrogen, the peak intensity at 1635 cm^{-1} was higher than that at 1600 cm^{-1}. The relative intensity at 1635 cm^{-1} was drastically reduced when the 260−22 film was prepared under identical conditions, except for the use of THF, a good solvent for both PS and PCEMA, in preparing the 260−22 coating solution (Figure 5). Since the peaks at 1635 and 1600 cm^{-1} are characteristic of the stretching motions of the aliphatic C=C of CEMA and the phenyl rings of PS and

Table 2. Characterization of PS-*b*-PCEMA by Static Light Scattering

lab code	w_{PS}	ν (mL/g)	$\bar{M}_w$* (g/mol)	$\bar{M}_w$ (g/mol)	$10^{-2}n$	$10^{-1}m$	R_G* (Å)
800−60	0.85	0.111	10.0×10^4	10.3×10^4	8.4	6.1	142
330−23	0.83	0.111	3.4×10^4	3.5×10^4	2.75	2.3	
400−33	0.80	0.110	4.4×10^4	4.5×10^4	3.5	3.5	
120−10	0.80	0.110	1.62×10^4	1.67×10^4	1.28	1.3	
200−16	0.80	0.110	2.97×10^4	3.1×10^4	2.35	2.4	
1200−150	0.79	0.110	24.6×10^4	25.4×10^4	19.4	20.3	201
1600−200	0.79	0.110	28.8×10^4	29.8×10^4	22.6	24.1	206
260−22	0.79	0.110	2.70×10^4	2.79×10^4	2.11	2.3	
400−50	0.77	0.110	4.1×10^4	4.2×10^4	3.1	3.8	
800−100	0.76	0.110	16.5×10^4	17.1×10^4	12.5	15.8	188
600−75	0.74	0.110	10.6×10^4	11.0×10^4	7.8	11.1	132
400−67	0.73	0.109	6.9×10^4	7.2×10^4	5.0	7.4	120
250−45	0.68	0.109	3.4×10^4	3.6×10^4	2.33	4.4	
400−100	0.65	0.108	6.5×10^4	6.8×10^4	4.3	9.1	134
250−60	0.58	0.107	4.7×10^4	5.0×10^4	2.78	7.9	
800−200	0.58	0.107	22.6×10^4	23.7×10^4	13.2	38	206
600−150	0.56	0.107	15.9×10^4	16.7×10^4	9.0	28.1	184
200−50	0.55	0.107	4.1×10^4	4.3×10^4	2.29	7.4	
300−150	0.42	0.104	6.7×10^4	6.9×10^4	2.78	15.4	

Table 3. Data of Polymer Adsorption by Silica ($f_{cp} = 0.86$)

lab code	σ_∞ (μg/cm^2)	$\rho_\infty \times 10^{-12}$	ρ_∞/ρ*	β	$m^{-(17/23)}\beta^{-(10/23)}$	e (Å)	$m^{(6/23)}\beta^{-(10/23)}$
			van der Waals−Buoy Regime				
330−23	0.37	6.4	5.6	6.06	0.0450	6.3	1.04
800−60	0.48	2.8	9.3	7.27	0.0202	7.3	1.23
400−33	0.44	5.9	6.8	5.68	0.0340	8.7	1.19
120−10	0.35	12.6	4.4	5.10	0.0740	7.0	0.96
200−16	0.35	6.9	5.0	5.40	0.0459	7.2	1.10
1200−150	0.39	0.92	8.2	6.58	0.0087	8.1	1.76
1600−200	0.45	0.91	9.7	6.63	0.0076	9.5	1.84
260−22	0.35	7.6	4.8	5.17	0.0482	7.5	1.11
800−100	0.31	1.09	5.8	5.75	0.0111	7.4	1.75
600−75	0.34	1.86	5.6	5.15	0.0151	8.9	1.68
400−67	0.36	3.1	5.4	4.86	0.0209	9.8	1.55
400−100	0.33	2.95	4.3	3.96	0.0196	11.6	1.78
800−200	0.38	0.84	4.8	3.81	0.0069	15.9	2.64
600−150	0.38	1.37	4.9	3.54	0.0089	16.6	2.51
400−50	0.50	7.2	7.2	5.06	0.0336	11.8	1.28
			Buoy-Dominated Regime				
250−45	0.46	7.8		3.96	0.0335		
250−60	0.50	6.1		3.29	0.0236		
200−50	0.52	7.3		3.03	0.0257		
300−150	0.77	6.7		2.36	0.0174		

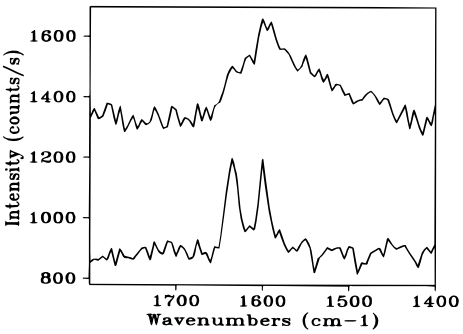

Figure 5. Surface-enhanced Raman spectra of 260−22 films on silica surfaces prepared by evaporating 260−22 solutions in THF (top) and CP/THF (bottom) with $f_c = 0.86$.

PCEMA, respectively, we conclude that there are more CEMA units on SiO_2 surfaces when the coating solution was prepared from the poor solvent, i.e. CP/THF, for PCEMA. Similar results were obtained for 300−150, 400−50, 800−200, and 800−60.

Unfortunately, SERS cannot give quantitative information about the amount of PCEMA anchored on silver surfaces, as both PCEMA and PS contain phenyl rings. The presence of the peak at 1600 cm^{-1} does not necessarily suggest PS adsorption. Only by combining with the adsorption data of diblocks and PS homopolymers, we can conclude that PCEMA must be the dominant anchoring species on silica when deposited out from CP/THF mixtures.

Films of PS-*b*-PCEMA on SiO_2 surfaces prepared using our method for the SERS studies were not monolayer films. After the withdrawal of a SiO_2 substrate from a coating solution, a thin layer of the coating solution would be left on it. The evaporation of the solvent would leave behind a polymer film. When THF was used as the solvent, this would probably have been the only polymer layer on the solid substrate. When CP/THF was used as the solvent, a polymer brush should have been in equilibrium with the coating solution before the withdrawal of the substrate. As the substrate was not rinsed with CP/THF immediately after the substrate was withdrawn, the final film on SiO_2 could have consisted of a brush layer at the bottom and a layer resulting from the solution evaporation at the top. Or the brush and the top layer might have been mixed. We did not study monolayers by rinsing the overlayer off with CP/THF, in which the brush layer is stable but not the top layer, because the signal to noise ratio of the SERS spectra of a monolayer was too low. Regardless of the structure of the polymer film or films formed on silica, the final conclusion that there were more CEMA groups on silica surfaces when a diblock deposited out from CP/THF should not have been affected.

PS-*b*-PCEMA Brush Formation on Silica Surfaces. For PS-*b*-PCEMA brush formation under our conditions, two criteria must be met. First, a diblock must be adsorbed via the PCEMA block. This has been demonstrated by the evidence presented in the last subsection. Then, the surface coverage should be sufficiently high so that chains of the PS layer are stretched due to repulsion between neighboring chains. We could not determine the magnitude of PS chain stretching. Instead, we show that PS chains in the buoy layer are crowded. In a crowded PS layer, the chains should be extended.

Experimental silica surface coverages, σ_∞, are shown in Table 3. The surface coverage, ρ_∞, in terms of the number of chains per unit surface, was calculated using

$$\rho_\infty = \frac{\sigma_\infty}{M_w} N_A \tag{8}$$

where N_A is Avogadro's constant.

The critical surface coverage at which the chains of the PS buoy layer begin to overlap can be calculated using

$$\rho^* = \frac{1}{\pi R_{GPS}{}^2} \tag{9}$$

where R_{GPS} is the radius of gyration of the PS block in a dilute solution. We did not determine R_{GPS} for our samples in CP/THF with $f_c = 0.86$. Instead, we used

$$R_{GPS} = 1.86 n^{0.595} \quad (\text{Å}) \tag{10}$$

which is valid for PS in toluene,[16] to estimate the ρ^* values. Since ρ_∞/ρ^* values for our samples are all considerably larger than 1 (Table 3), we deduce that neighboring chains repel one another and that the PS chains are stretched.

Verification of the Theory of Marques et al. for the van der Waals−Buoy Regime. All of our polymers existed as micelles in CP/THF with $f_c = 0.86$, as characterized by the bluish tinge of their solutions. Then, the polymers should be adsorbed by silica in the brush conformation. Furthermore, our polymers were designed to have relatively large β values. Under these conditions, ρ_∞ should follow the scaling relation derived by Marques et al. for polymer adsorption from a micellar solution in the van der Waals−buoy regime:

$$a^2 \rho_\infty \approx (A/kT) m^{-(17/23)} \beta^{-(10/23)} \tag{11}$$

where a denotes the effective length of a PS repeat unit, kT the thermal energy, and A a negative Hamaker constant characteristic of the interaction between silica and the solution phase separated by a PCEMA anchoring layer. A plot of ρ_∞ versus $m^{-(17/23)}\beta^{-(10/23)}$ is illustrated in Figure 6. Data points of the 250−45, 250−60, 200−50, and 300−150 samples are obviously off the best fit line to the other data points. This can be explained by their relatively small β values and the possibility that their adsorption behavior should be explained by a scaling relation in the buoy-dominated regime.[9,10] Excluding the data for 250−45, 250−60, 200−50, and 300−150, the best fit to the other data points yielded

$$10^{-12} \rho_\infty = 173 m^{-(17/23)} \beta^{-(10/23)} - 0.45 \tag{12}$$

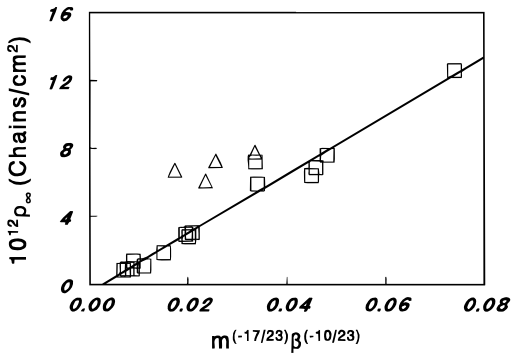

Figure 6. Plot of ρ_∞ vs $m^{-(17/23)}\ \beta^{-(10/23)}$ for PS-*b*-PCEMA adsorption by silica from CP/THF with $f_c = 0.86$. The straight line denotes the best fit to the data points represented by □'s. Adsorption data of 250−45, 250−60, 200−50, and 300−150 are denoted by △'s.

with a correlation coefficient of 0.984. This represents the first experimental verification of the scaling relation of Marques et al. for the van der Waals−buoy regime.[10]

The intercept of the straight line in Figure 6 is slightly negative. There can be several causes for this. First, the scaling relation of Marques et al. was derived by making many approximations. When the neglected terms are included, the exact relation may have a nonzero intercept. Second, Marques et al. derived the scaling relations based on the assumption that a single solvent was used to prepare the coating solution. Our experiments did not correspond exactly to the theoretically analyzed situation, as a binary solvent mixture was used. Third, silica was coated from a stirred diblock solution and the coated silica was subsequently separated from the supernatant by centrifuging. The shearing field caused by both the rotating magnetic bar and centrifuging may have led to the dissociation of some chains from polymer brushes, a situation not considered by Marques et al. Fourth, we did not determine σ_∞ from adsorption isotherms and therefore σ_∞ determined using our method may be slightly lower than the true σ_∞. Lastly, the ∼48 h equilibration time between silica and the coating solution could have been the culprit, as the theoretical analysis of Ligoure and Liebler[17] suggests that it can take a long time to attain adsorption equilibrium of a diblock copolymer. Our adsorption kinetic results, however, demonstrate that the error caused by the use of this equilibration time should be small.

Comparing eqs 12 and 11 and assuming an a value of 4 Å and $T = 298$ K, we calculated an A value of 2.8×10^{-23} J.

Crossover from the van der Waals−Buoy Regime to the Buoy-Dominated Regime. The theory of Marques et al. predicts a crossover from the van der Waals−buoy regime to the buoy-dominated regime upon decreasing β. The crossover β^* value seems to be in the neighborhood of 3.5 for PS-*b*-PCEMA adsorption onto silica. The exact β^* value depended on the polymer used. Polymer 600−150, for example, possesses a β value of 3.54 and its adsorption data still fell on the best fit line to the other data points. Sample 250−45 has a β value of 3.96 and its adsorption data are already far off from the best fit line. Thus, the β^* value appeared to be smaller for samples with higher molar masses. This trend is, however, not conclusive at this time and needs further experimental confirmation. Also, the solvency power of CP/THF with $f_c = 0.86$ for PS is questionable here. If the mixture is not a good solvent

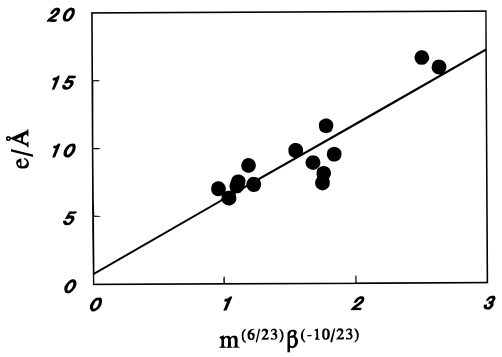

Figure 7. Plot of e vs $m^{6/23}\beta^{-(10/23)}$ for PS-*b*-PCEMA adsorption by silica from CP/THF with $f_c = 0.86$. The e values of 400−50, 250−45, 250−60, 200−50, and 300−150 brushes were not included in this graph.

for PS, β should not be defined by eq 3, as R_{GPS} would have a weaker dependence on n.

Scaling Behavior of the PCEMA Thickness. Assuming a density, d, of 1.00 g/cm^3 for the anchoring layer and that it is essentially free of solvent as assumed in most theoretical models, the thickness, e, of the anchoring layer can be calculated using

$$e = \frac{w_{PCEMA}\sigma_\infty}{d} \tag{13}$$

where w_{PCEMA} is the mass fraction of the PCEMA block of a diblock. Using eq 13, we calculated e for all of our samples (Table 3). To be more realistic, one can also assume a uniform swelling factor, α, for the PCEMA layer, as THF may be preferentially sorbed by PCEMA. In that case, the PCEMA thickness would be αe.

The PCEMA thickness, e or αe, should scale according to[10]

$$e \propto m^{6/23}\beta^{-(10/23)} \tag{14}$$

The overall trend of increasing e with $m^{6/23}\beta^{-(10/23)}$ was obeyed by our data, but our data were not well fitted by eq 14 (Figure 7). One reason is that our e values only spanned a very narrow range which accentuated the deviation of individual e values from the best fit line. Also, the assumption that the anchoring PCEMA layers of brushes formed from different polymers are not swollen or are swollen to the same degree may be erroneous. The no-swelling assumption is nonrealistic, as THF is a good solvent for PCEMA and some sorption of THF by the PCEMA layer must have occurred. Then, the assumption that an identical degree of swelling exists might be wrong, as the number of CEMA units m changes from 13 to 383 for different diblocks. Such a change in m would correspond to a pronounced change in the properties of PCEMA, including its ability to sorb THF.

Surface Coverages of Ag−Ni Spheres at Diblock Adsorption Equilibrium. Using the conditions described in the Experimental Section, surface coverages, σ_∞, of Ag−Ni spheres by different diblocks were determined. Inserting the σ_∞ values into eq 8, we calculated the surface coverages ρ_∞ (Table 4). When plotted against $m^{-(17/23)}\beta^{-(10/23)}$, the ρ_∞ values could be fitted by a quadratic function:

$$10^{-12}\rho_\infty = 5.65 \times 10^3 m^{-(34/23)}\beta^{-(20/23)} + 193 m^{-(17/23)}\beta^{-(10/23)} - 0.21 \tag{15}$$

with a correlation coefficient of 0.983 (Figure 8).

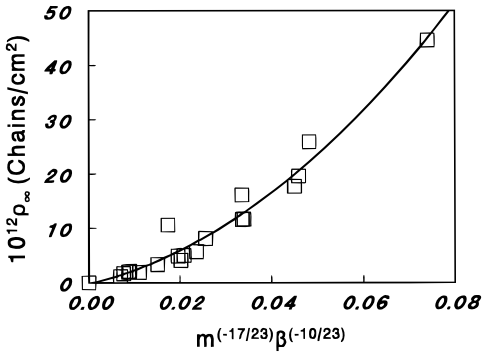

Figure 8. Plot of ρ_∞ vs $m^{-(17/23)}\beta^{-(10/23)}$ for PS-*b*-PCEMA adsorption by silver from CP/THF with $f_c = 0.96$. The solid curve represents the best fit to the data points represented by □'s. Adsorption data of 260−22, 250−45, and 300−150 are denoted by △'s.

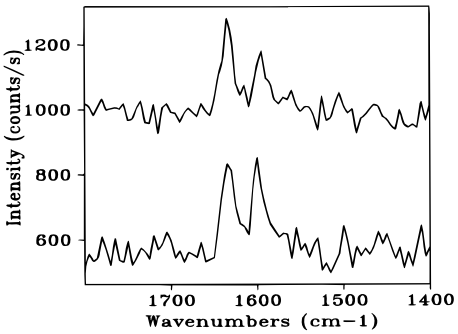

Figure 9. Surface-enhanced Raman spectra of 800−200 films on silver surfaces prepared by evaporating 800−200 solutions in THF (bottom) and CP/THF with $f_c = 0.96$ (top).

Table 4. Data of Polymer Adsorption by Silver (f_{cp} = 0.96)

lab code	σ_∞ (μg/cm^2)	$\rho_\infty \times 10^{-12}$
330−23	1.02	17.7
800−60	0.71	4.1
400−33	0.87	11.7
120−10	1.24	44.6
200−16	1.00	19.6
1200−150	0.84	1.98
1600−200	0.83	1.69
400−50	0.82	11.6
800−100	0.54	1.90
600−75	0.61	3.3
400−67	0.60	5.0
400−100	0.55	4.9
250−60	0.47	5.7
800−200	0.52	1.15
600−150	0.58	2.09
200−50	0.58	8.1
260−22	1.20	25.9
250−45	0.95	16.1
300−150	1.22	10.6

Comparing Figures 8 and 6, it can be seen that ρ_∞ of samples with small $m^{-(17/23)}\beta^{-(10/23)}$ values are comparable with those obtained using silica as the adsorbent. For those samples with small m and large asymmetric ratios β, the ρ_∞ values are much larger than those observed on silica.

Performing SERS studies of 800−200 and 260−22 yielded the spectra shown in Figures 9 and 10. By changing the solvent used in preparing coating solutions of 800−200 from THF to CP/THF with $f_c = 0.96$, the ratio between the intensities of the SERS peaks at 1635 and 1600 cm^{-1} increased considerably, in agreement with the SERS results of 800−200 obtained on silica. When a similar experiment was done for 260−22, the

increase in the signal intensity at 1635 cm^{-1} is much less pronounced (Figure 10). Furthermore, the intensity ratio for peaks at 1635 and 1600 cm^{-1} is much less than that observed when SiO_2 was used as the substrate (Figure 5).

Thus, the logical explanation for the above adsorption and SERS results is that polymers with large m and small β values were mainly adsorbed on silver via the PCEMA block in the brush conformation and that both the PS and PCEMA blocks can be adsorbed by silver for samples with small m and large β values. This is possible as the block of a diblock copolymer which is adsorbed is determined not only by the magnitude of the interaction between a repeat unit in a chain with a substrate but also by the number of repeat units in a chain. As the number of repeat units increases, the number of possible anchoring sites increases. In CP/THF with $f_c = 0.96$, the anchoring strength of a CEMA unit may be stronger than that of a styrene unit, which makes CEMA the major anchoring groups when the β values are small. As β increased, the PS chains become much longer than the PCEMA chains. It is the excess number of repeat units or potential anchoring sites of PS which makes PS competitive with PCEMA in occupying surface sites. The simultaneous PS and PCEMA adsorption became particularly favorable for samples with large β and small m values, as decreasing m values will decrease the driving force for phase separation between the PS and PCEMA blocks. The simultaneous adsorption of PS and PCEMA destroys the two-layered (PCEMA anchoring layer and then PS buoy layer) structure of a polymer brush. Instead, a homogenized diblock film or an adsorbed micellar layer may form on a silver substrate, which led to extraordinarily large ρ_∞ values.

That PS does adsorb on silver surfaces was unambiguously concluded from the study of the adsorption of a PS homopolymer ($\bar{M}_w = 9.0 \times 10^4$ g/mol and $\bar{M}_w/\bar{M}_n = 1.04$) from CP/THF with $f_c = 0.96$. While the surface coverage of silica by this polymer was only 0.040 $\mu g/cm^2$, that of silver was 0.15 $\mu g/cm^2$.

The other possible reason for the curved line in Figure 8 is that different adsorption regimes might have existed for different samples. When β are small and m are large, the samples exist as micelles at the concentration ~1.0 mg/mL in CP/THF mixtures with $f_c = 0.96$, as suggested by the bluish tinge of their solutions. We could not visually discern micelle formation from the samples with large β and small m values. Thus, the adsorption of polymers with large β and small m values might have occurred from unimer solutions, and that of polymers with small β and large m values might have occurred from micellar solutions. We did not use higher concentrations, ~10 mg/mL, of the polymers to ensure micelle formation from all samples, as the use of a much more concentrated solution would have made the concentration decrease after polymer adsorption negligible. Much less polymer was adsorbed by Ag−Ni spheres than by silica as the specific surface area of Ag−Ni spheres was much lower.

In conclusion, PS-*b*-PCEMA samples in CP/THF with $f_c = 0.96$ were not necessarily adsorbed by Ag−Ni spheres in the brush conformation. Then, the polymer coating solutions could have been unimer or micellar solutions, which depended on the β and m values. Thus, it was not surprising that the theory of Marques et al. could not be used to treat the data of PS-*b*-PCEMA adsorption by silver in CP/THF with $f_c = 0.96$.

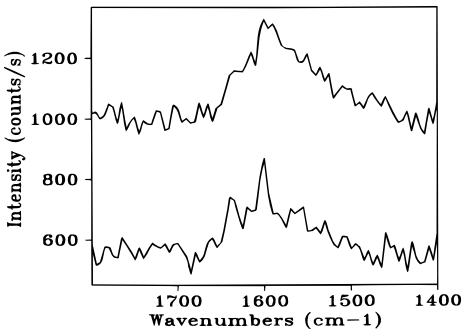

Figure 10. Surface-enhanced Raman spectra of 260−22 films on silver surfaces prepared by evaporating 260−22 solutions in THF (top) and CP/THF with $f_c = 0.96$ (bottom).

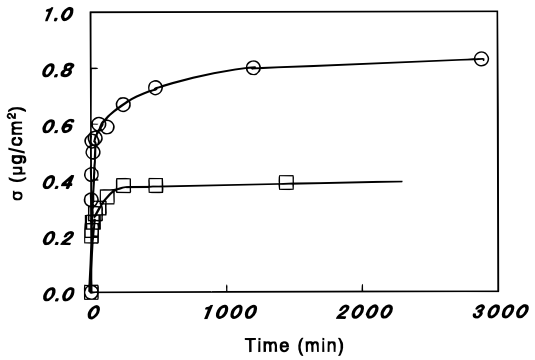

Figure 11. Amounts of 1600−200 adsorbed by silica (□) and silver (○) as a function of adsorption time. For coating silica, a 14 mg/mL 1600−200 solution in CP/THF with 86% CP was used. For coating silver, a 1.0 mg/mL 1600−200 solution in CP/THF with 96% CP was used.

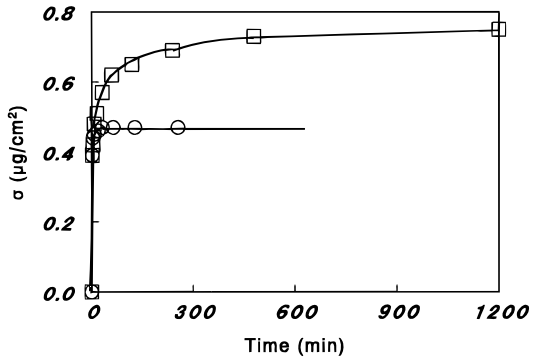

Figure 12. Amounts of 400−50 adsorbed by silica (○) and silver (□) as a function of adsorption time. For coating silica, a 10 mg/mL 400−50 solution in CP/THF with 86% CP was used. For coating silver, a 1.0 mg/mL 400−50 solution in CP/THF with 96% CP was used.

Rate of PS-*b*-PCEMA Adsorption by Silica. In order to establish the time scale at which the diblock adsorption reaches equilibrium, we determined the kinetics of 1600−2000 and 400−50 adsorption by silica, and the results are shown in Figures 11 and 12. The longer time taken to reach adsorption equilibrium for the higher molar mass sample 1600−200 is expected. Our kinetic data suggest that the equilibration time of 48 h used in determining σ_∞ should have been sufficient for all our samples, as 1600−200 is the sample with the highest molar mass.

Kinetics of Polymer Adsorption by Ag−Ni Spheres. We also carried out the kinetic study of 1600−200 and 400−50 adsorption on Ag−Ni spheres, and the results are shown in Figures 11 and 12 for comparison with those obtained using silica as the adsorbent. When Ag−Ni spheres were used as the

adsorbent, higher rates, $d\sigma/dt$, of 1600−200 and 400−50 adsorption, higher equilibrium surface coverages, and longer adsorption equilibrium times were observed compared to the case when silica was used. Despite the longer equilibrium time, 48 h (Figures 11 and 12) looks sufficient for determining σ_∞ of our samples on silver surfaces.

The higher adsorption rates, the ultimately higher surface coverages, and the longer construction times for the 1600−200 and 400−50 layers can all be explained by a more favorable interaction between the diblocks and silver than that between the diblocks and silica. A more favorable interaction between a chain and a substrate means that the adsorption process is more downhill in energy. That an energetically more favored process may have a lower activation energy and thus a faster rate is expected. This is particularly true at short adsorption times when the surface coverages are low, the adsorbed chains are far apart, and the kinetics of polymer chain adsorption is mainly governed by the adsorption energy of a diblock copolymer. That a more favorable polymer/substrate interaction increases the equilibrium surface coverage of a substrate by a polymer is expected. That a denser layer takes a longer time to build up can be understood as follows.[17] Initially, the rate of polymer chain adsorption is governed by the interaction energy between a polymer and a substrate. As the adsorbed polymer layer becomes dense, new chains have to overcome the energy barrier created by chains already adsorbed and squeeze into the existing layer to be incorporated. The rate of polymer adsorption at this stage is thus mainly determined by the energy barrier derived from the existing adsorbed layer. The denser this adsorbed layer is, the slower the incorporation of new chains. Thus, a higher equilibrium surface coverage takes a longer time to construct.[17]

The improved interaction between the diblocks and silver may be characteristic of the polymers and the substrate studied. Then, different CP contents, i.e. 86 and 96% when coating silica and silver, respectively, may have also contributed to this. When CP content increased, the solvent mixture became poorer for the PCEMA block, and the thermodynamic driving force for PCEMA to deposit out on silver increased.

IV. Conclusions

We synthesized and characterized 19 PS-*b*-PCEMA samples with various m and β values. In CP/THF, the diblocks were adsorbed by silica mainly via the PCEMA block in the brush conformation, as revealed by our surface-enhanced Raman results and PS and PS-*b*-PCEMA adsorption data. On silver surfaces, only PS-*b*-PCEMA diblocks with sufficiently large m and small β values were mainly adsorbed via the PCEMA block. Otherwise, PS also adsorbed on the silver surface. The different behaviors on silica and silver could be partially due to the substrate effect. Also, the solvent composition difference used could also be the cause.

Of the 19 surface coverages of silica determined, 15 could be fitted by the scaling relation of Marques et al. for diblock adsorption from micelle solutions in the van der Waals−buoy regime. This represents the first experimental observation of such a relationship. The adsorption data of another four polymers did not follow this relation, probably because their β values were too low and have thus crossed the boundary between the van der Waals−buoy and the buoy-dominated regimes.

Acknowledgment. We would like to acknowledge the NSERC Strategic Grant program for financially sponsoring this research. Dr. R. Kydd is thanked for showing and allowing J.D. to use his Raman spectrometer.

References and Notes

(1) Milner, S. *Science* **1991**, *251*, 905.
(2) Halperin, A.; Tirrell, M.; Lodge, T. P. *Adv. Polym. Sci.* **1992**, *100*, 31.
(3) Gast, A. P. In *Scientific Methods for the Study of Polymer Colloids and Their Applications*; Candau, F., Ottewill, R. H., Eds.; Kluwer Academic Publishers: Amsterdam, 1990.
(4) Liu, G. In *The Polymeric Materials Encyclopedia—Synthesis, Properties, and Applications*; Salamone, J. C., Ed.; CRC Press: Boca Raton, FL, in press.
(5) Bossé, F.; Schreiber, H. P.; Eisenberg, A. *Macromolecules* **1993**, *26*, 6447.
(6) Parsonage, E.; Tirrell, M.; Watanabe, H.; Nuzzo, R. G. *Macromolecules* **1991**, *24*, 1987.
(7) Watanabe, H.; Tirrell, M. *Macromolecules* **1993**, *26*, 6455.
(8) Stouffer, J. M.; McCarthy, J. *Macromolecules* **1988**, *21*, 1204.
(9) Tao, J.; Guo, A.; Liu, G. *Macromolecules* **1996**, *29*, 1618.
(10) Marques, C.; Joanny, J. F.; Leibler, L. *Macromolecules* **1988**, *21*, 1051.
(11) Liu, G.; Smith, C. K.; Hu, N.; Tao, J. *Macromolecules* **1996**, *29*, 220.
(12) Hill, Wieland; Rogalla, D.; Klockow, D. *Anal. Methods Instrum.* **1993**, *1*, 89.
(13) Guo, A.; Tao, J.; Liu, G. *Macromolecules* **1996**, *29*, 2487.
(14) Pockrand, I. *Surface Enhanced Raman Vibrational Studies at Solid/Gas Interfaces*; Springer-Verlag: Berlin, 1984.
(15) Tsai, W. H.; Boerio, F. J.; Clarson, S. J.; Parsonage, E. E.; Tirrell, M. *Macromolecules* **1991**, *24*, 2538.
(16) Higo, Y.; Ueno, N.; Noda, I. *Polym. J.* **1983**, *15*, 367.
(17) Ligoure, C.; Liebler, L. *J. Phys. (Paris)* **1990**, *51*, 1313.

MA960277C